

Plastic Instability of Rate-Dependent Materials - A Theoretical Approach in Comparison to FE-Analyses -

Christian Keller¹, Uwe Herbrich¹

¹Bundesanstalt für Materialforschung und -prüfung
12200 Berlin, Germany

1 Abstract

The condition for plastic instability is a material characteristic and defines the onset of necking in tensile tests. In large deformation problems of ductile materials it is fundamental to determine the strain at which necking starts as well as the post-necking behaviour in the instability region properly. For verification purposes of material models, usually results of numerical analyses are compared to experimental outcomes. For tensile tests with ductile materials under dynamic loading, it is challenging to obtain comparable experimental and numerical results in terms of the onset of necking and the post-critical deformation behaviour. This paper focuses on the derivation of a theoretical criterion describing the plastic instability in rate-dependent materials based on the time variation of the strain gradient in a tensile specimen under isothermal conditions. We examine the influence of various constitutive equations on the theoretical stability condition predicted by different multiplicative as well as additive approaches. For multiplicative relations, the results indicate that the onset of necking is, in principle, independent of the strain rate, whereas for the considered additive relation, the dynamic necking strain must decrease with increasing strain rate. In conclusion, the theoretical stability condition is related to results from finite element simulations of dynamic tensile tests with various loading rates. It is shown that the simulated and the theoretical predicted onset of plastic instability agree reasonably.

2 Introduction

In finite element (FE) simulations of dynamic events, the accuracy of numerical results strongly depends on the quality of the material models and parameters used. Material characteristics identified in static tests are not suitable or are of limited suitability for the description of the deformation behaviour of components and structures under dynamic loading. On this account, it is necessary to determine material properties in dynamic tests and to provide reliable input data for numerical simulations, e.g. by means of rate-dependent material models or flow curves. This can be achieved, for instance, by carrying out tensile tests with different loading rates, which, – statically or dynamically – are characterised by a material dependent plastic instability and necking of the specimens. In certain applications, the evaluation of tensile tests in the range between initial plastic deformation and the uniform elongation, the strain at which necking starts, is sufficient. However, for the consideration of large deformation problems, it is essential to evaluate and establish material properties for the plastic deformation behaviour beyond the uniform elongation. The tensile testing of metallic materials is a standard method and the static mechanical properties which can be determined at room temperature are defined in the ISO 6892-1 standard [1]. According to that, a test is considered (quasi-)static for a nominal strain rate of $\dot{\epsilon}_n \leq 8 \cdot 10^{-3} \text{ s}^{-1}$. In this paper, the index n denotes nominal or engineering quantities. However, many engineering materials exhibit a positive strain rate effect, i.e., the flow stress increases with increasing strain rate. In the ISO 26203-2 standard [2] dynamic tensile testing is defined for nominal strain rates from $10^{-2} \text{ s}^{-1} \leq \dot{\epsilon}_n \leq 10^3 \text{ s}^{-1}$ at room temperature. Though, due to adiabatic heating of the specimen, at higher nominal strain rates ($\dot{\epsilon}_n \geq 10 \text{ s}^{-1}$) it is impossible to conduct isothermal tests.

The main drawback of static as well as dynamic tension tests is the necking of the specimen due to a plastic instability during the tensile deformation. Up to the uniform elongation at which the instability arises, the stress distribution in the specimen can be considered as uniaxial. Therefore, the experimental data can directly be evaluated and provided as true stress and true plastic strain curves for the description of the constitutive behaviour. Once necking occurs, the assumption of a uniaxial state of stress is invalid. Moreover, the strain localizes in the neck and in dynamic tests the local increase of the strain rate as well as the temperature are significant. Since the plastic instability that causes the necking is a material characteristic, it is essential to be considered regarding the constitutive relations in dynamic plasticity.

3 Constitutive Equations in Dynamic Plasticity

In dynamic plasticity, strain hardening, strain rate dependence and temperature determine the flow stress of engineering materials. In ductile materials, elastic strains are small compared to the necking or failure strains and can therefore be neglected. Assuming that the true stress σ is a unique function of true plastic strain ε_{pl} , true plastic strain rate $\dot{\varepsilon}_{pl}$ and absolute temperature T , the constitutive equation is given by:

$$\sigma = f(\varepsilon, \dot{\varepsilon}, T) \quad \text{with } \varepsilon \approx \varepsilon_{pl} \text{ and } \dot{\varepsilon} \approx \dot{\varepsilon}_{pl} \quad (1)$$

Where the true strain ε and the true strain rate $\dot{\varepsilon}$ as well as the temperature are assumed to be independent quantities. Based on that, there are two fundamental approaches describing dynamic plasticity in engineering materials by relating the strain-dependent term multiplicatively or additively to strain rate and temperature-dependent functions.

3.1 Multiplicative decomposition

The first group of approaches describing the flow stress assumes a multiplicative relation between independent functions:

$$\sigma(\varepsilon, \dot{\varepsilon}, T) = f_1(\varepsilon) f_2(\dot{\varepsilon}) f_3(T) \quad (2)$$

One of the most common representative of multiplicative relations is the constitutive equation suggested by Johnson and Cook [3], which has been widely used by numerous authors for various applications in order to describe the strength of different materials in numerical simulations of dynamic events, e.g. [4, 5, 6]. The Johnson-Cook (JC) model expresses the true stress as a function of strain hardening, strain rate hardening and thermal softening as follows:

$$\sigma(\varepsilon, \dot{\varepsilon}, T) = [A + B \cdot \varepsilon^n] \cdot \left[1 + C \cdot \ln\left(\frac{\dot{\varepsilon}}{\dot{\varepsilon}_0}\right)\right] \cdot [1 - T^{*m}] \quad \text{with } T^* = \frac{T - T_r}{T_m - T_r} \quad (3)$$

Where A, B, C, n and m are material constants, $\dot{\varepsilon}_0$ is a true reference strain rate for normalization and T^* is the modified temperature defined by the melting temperature T_m of the material and a reference temperature T_r , which must be chosen as the lowest temperature of interest. The modified temperature is valid in the range $T_r \leq T \leq T_m$ and for isothermal conditions ($T = const.$) the JC-model reduces to:

$$\sigma(\varepsilon, \dot{\varepsilon}) = [\hat{A} + \hat{B} \cdot \varepsilon^n] \cdot \left[1 + C \cdot \ln\left(\frac{\dot{\varepsilon}}{\dot{\varepsilon}_0}\right)\right] \quad (4)$$

with

$$\hat{A} = A \cdot [1 - (T^{*m})_{T=const}] \quad \text{and} \quad \hat{B} = B \cdot [1 - (T^{*m})_{T=const}]. \quad (5)$$

Another widely used multiplicative approach is the constitutive relation proposed by Cowper and Symonds [7], which originally described the strain rate dependence of the upper yield stress but later was generalized as a strain hardening model, assuming the rate-dependence of the material to be governed by the following equation:

$$\sigma(\varepsilon, \dot{\varepsilon}) = \sigma_s(\varepsilon) \cdot \left[1 + \left(\frac{\dot{\varepsilon}}{D}\right)^{1/p}\right] \quad (6)$$

In the Cowper-Symonds (CS) model, Eq.(6), the dynamic behaviour is represented by scaling up a general quasi-static true stress- true strain relation $\sigma_s(\varepsilon)$ by a power law with the Cowper-Symonds parameters D and p . Adiabatic effects and thermal softening are not considered, but due to its simplicity and its sufficient accuracy in many engineering application, the CS model is one of the most cited and applied relations in dynamic plasticity.

3.2 Additive decomposition

The second group of approaches, describing the flow stress of engineering materials, assumes an additive scheme and is expressed in general terms as:

$$\sigma(\varepsilon, \dot{\varepsilon}, T) = h_1(\varepsilon) + h_2(\dot{\varepsilon}, T) \quad \text{assuming } \exists h_2^{-1}(\bullet) \quad (7)$$

Where h_2^{-1} is the inverse function of h_2 . The structure in Eq.(7) is often denoted as ‘overstress’ hypothesis. Herein, the true stress is separated in two parts, the strain-dependent function $h_1(\varepsilon)$ describing the static true stress-true strain relation, i.e. $h_1(\varepsilon) = \sigma_s(\varepsilon)$, and the rate- and temperature-dependent overstress function $h_2(\dot{\varepsilon}, T)$. Rearranging terms in Eq.(7) yields:

$$\dot{\varepsilon} = h_2^{-1}(\sigma(\varepsilon) - \sigma_s(\varepsilon), T) \quad \text{with } \sigma(\varepsilon) \geq \sigma_s(\varepsilon) \quad (8)$$

One of the first overstress approximations were proposed by Sokolovsky and Malvern [8, 9]. Assuming, that the plastic strain rate depends only on the overstress $\Delta\sigma = \sigma - \sigma_s$ without consideration of strain and temperature influence on $\Delta\sigma$, Eq.(8) reduces to:

$$\dot{\varepsilon} = g(\Delta\sigma) \quad (9)$$

As a special case of the more general relation in Eq.(9), Cowper and Symonds [7] considered the stress-strain relation in the plastic range introducing a strain rate effect:

$$\dot{\varepsilon} = g(\Delta\sigma) = \tilde{D} \cdot (\Delta\sigma)^{\tilde{p}} \quad (10)$$

Inverting Eq.(10) results in the constitutive equation:

$$\sigma(\varepsilon, \dot{\varepsilon}) = \sigma_s(\varepsilon) + \left(\frac{\dot{\varepsilon}}{\tilde{D}}\right)^{1/\tilde{p}} \quad (11)$$

The relation in Eq.(11) is used for the studies in this paper, that are exemplarily discussed for additive approaches describing the flow stress in dynamic plasticity.

3.3 Determination of model parameters under isothermal conditions for a ductile steel

The main subject in this paper is the discussion of plastic instability in rate-dependent, ductile materials, formulated with the three different constitutive equations introduced before: the models proposed by Johnson-Cook and Cowper-Symonds as well as the overstress hypothesis. In contrast to real dynamic events, the thermal softening due to adiabatic heating is neglected in the analytical considerations and the numerical simulations. Hence, the constitutive behaviour should be formulated using the isothermal equations in Eq.(4), Eq.(6) and Eq.(11).

DH-36 structural steel is representatively selected as a ductile material. Its main field of application is in offshore and naval construction and its technical requirements as well its mechanical properties are standardized in the GL II-1-2 rule [10]. Nemat-Nasser and Guo [11] investigated the thermomechanical response of DH-36 steel over a wide range of strain rates ($10^{-3} \text{ s}^{-1} - 3,000 \text{ s}^{-1}$) and temperatures (77 K – 1,000 K). The experimental data displayed the high strength characteristic and good ductility of the material. Table 1 summarizes the Johnson-Cook material constants calibrated for DH-36 from [11]. Within this paper, the dependence of the true strain rate on the true stress is considered in a range from $\dot{\varepsilon}_{min} = 10^{-3} \text{ s}^{-1}$ up to $\dot{\varepsilon}_{max} = 500 \text{ s}^{-1}$, which are typical threshold values for quasi-static conditions and dynamic scenarios like crash or impact events, respectively. For the numerical simulations, the reference true strain rate has therefore to be lower and the JC material parameters A and B must be adapted. The reference strain rate is set to $\dot{\varepsilon}_0 = 10^{-6} \text{ s}^{-1}$ and the adjusted values are given in Table 2. Thus, the investigated constitutive behaviour is similar but not identical to the true stress-true strain relation of DH-36 and the flow curves presented in this paper must be considered as generic.

\tilde{A}	\tilde{B}	n	C	$\tilde{\varepsilon}_0$	m	T_r	T_m
1,020 MPa	1,530 MPa	0.4	0.015	1 s^{-1}	0.32	50 K	1,773 K

Table 1: Johnson-Cook model parameters calibrated for DH-36 steel by Nemat-Nasser and Guo [11]

A	B	n	C	$\dot{\varepsilon}_0$	m	T_r	T_m
844 MPa	1,266 MPa	0.4	0.015	10^{-6} s^{-1}	0.32	50 K	1,773 K

Table 2: Johnson-Cook model parameters adapted for a lower reference strain rate

Considering room temperature ($T = 296 \text{ K}$), the JC model reduces to Eq.(4) with $\hat{A} = 391.15 \text{ MPa}$ and $\hat{B} = 586.73 \text{ MPa}$. The quasi-static true stress and strain curve is then defined with Eq.(4) and $\dot{\varepsilon} = \dot{\varepsilon}_0$:

$$\sigma_s(\varepsilon) = [\hat{A} + \hat{B} \cdot \varepsilon^n] \quad (12)$$

Fig.1(a) shows the corresponding true stress versus true strain curves, displayed for four true strain rates $\dot{\varepsilon} = 10^{-6} \text{ s}^{-1}, 10^{-3} \text{ s}^{-1}, 1 \text{ s}^{-1}$ and 500 s^{-1} under isothermal conditions. In order to determine corresponding Cowper-Symonds parameters D and p , in Fig.1(b) initial yield stress values of $\ln(\Delta\sigma/\sigma_s)$ predicted by the Johnson-Cook model are plotted against $\ln(\dot{\varepsilon}/\dot{\varepsilon}_0)$ values. In this representation, the CS model with its power law in Eq.(6) is expressed by a straight line with the inverse of p defining the slope. It is seen from Fig.1(b), that the JC curve and the CS line can only coincide for two strain rates. As a first constraint, we define that both models must be exact at the highest strain rate of interest $\dot{\varepsilon}_{max}$. Secondly, the root mean square of $\ln(\Delta\sigma/\sigma_s)$ of both curves in the region of interest ($\dot{\varepsilon}_{min} < \dot{\varepsilon} < \dot{\varepsilon}_{max}$) must be minimized. The resulting straight line is displayed in Fig.1(b) and D and p can directly be derived from its linear equation.

Plotting Eq.(11) in $\ln(\Delta\sigma)$ against $\ln(\dot{\varepsilon}/\dot{\varepsilon}_0)$, the overstress hypothesis is also represented by a straight line and the parameter determination is carried out analogously. Mathematically, it can be shown, that both models have the same slope, i.e.:

$$\tilde{p} = p \quad (13)$$

Both, the Cowper-Symonds and the overstress parameters are adapted on the Johnson-Cook model within the region of interest and the determined values are summarized in Table 3. Figure 1 depicts flow curves defined by the Cowper-Symonds model and overstress hypothesis in comparison to the Johnson-Cook model within the range of $\dot{\varepsilon}_0 < \dot{\varepsilon}_{min} < \dot{\varepsilon} < \dot{\varepsilon}_{max}$, which will be used in the following sections to discuss plastic instability in rate-dependent materials.

\hat{A}	\hat{B}	n	D	\tilde{D}	$p = \tilde{p}$
391 MPa	587 MPa	0.4	$\exp(23.44) \text{ s}^{-1}$	$\exp(-62.08) \text{ s}^{-1}$	14.3

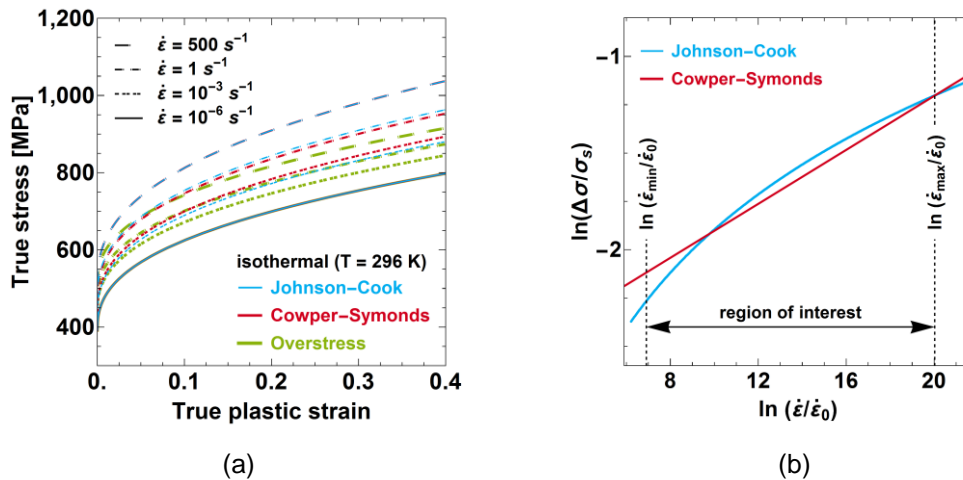
 Table 3: Cowper-Symonds and overstress hypothesis parameters, adapted on the Johnson-Cook model within the range of $\dot{\varepsilon}_{min} = 10^{-3} \text{ s}^{-1}$ up to $\dot{\varepsilon}_{max} = 500 \text{ s}^{-1}$ as region of interest


Fig.1: Comparison of flow curves for $\dot{\varepsilon} = 10^{-6} \text{ s}^{-1}, 10^{-3} \text{ s}^{-1}, 1 \text{ s}^{-1}$ and 500 s^{-1} defined with different constitutive equations (a) and logarithmic plot of normalized overstress against normalized strain rate at the initial yield stress of the Johnson-Cook model for the Cowper-Symonds parameter determination (b)

4 Criterion for plastic instability

4.1 Material with rate-independent stress-strain relation

In a static tensile test with ductile material, non-uniform plastic flow occurs when the uniaxial load reaches a maximum. At that point, the geometrical softening $dA/d\varepsilon$, i.e. the decrease in structural integrity due to the reduction of the cross-sectional area A of the tensile specimen, is equal or exceeds the rate of strain hardening of the material $d\sigma/d\varepsilon$. This results in a plastic instability and the development of a neck in the specimen over a length greater than its characteristic cross-section dimension. This so-called diffuse necking is shown schematically in Fig. 2 for a sheet metal specimen with rectangular cross-section. However, it must be emphasized that the plastic instability is a material characteristic and hence the strain or elongation at which necking occurs in a static test is not influenced by the specimen's geometry. Therefore, as expressed by Joun et al. [12], it is inappropriate to apply an analysis model with imperfections for a finite element analysis of a tensile test. Instead an ideal analysis model for simulation of the tensile test should be proposed.

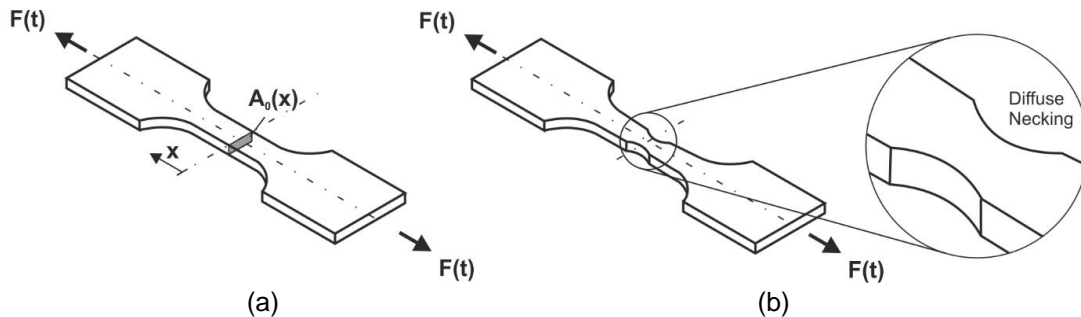


Fig.2: Schematic representation of a sheet-metal specimen with rectangular cross-section under uniaxial loading conditions: initial geometry (a) and geometry after onset of diffuse necking (b)

For a tensile test under uniaxial, static loading conditions and material with isotropic, rate-independent constitutive behaviour, the definition of a criterion for the onset of diffuse necking is straightforward. Assuming, that the force F is constant along the axis of the specimen, it can be defined:

$$F(t) = \sigma(x, t) \cdot A(x, t) = \text{const. in } x \quad (14)$$

The increase of tensile force dF , which is required to deform the specimen by $d\varepsilon$ is:

$$d_\varepsilon F = A d_\varepsilon \sigma + \sigma d_\varepsilon A \quad \text{with } d_\varepsilon \sigma > 0 \text{ and } d_\varepsilon A < 0 \quad (15)$$

Here and in the following, the abbreviations $d_\alpha(\bullet) := d(\bullet)/d\alpha$ and $\partial_\beta(\bullet) := \partial(\bullet)/\partial\beta$ are used. Furthermore, the equivalent representation of true (left side) and nominal (right side) quantities is applied consequently. For a stable deformation, the condition $d_\varepsilon F > 0$ must be satisfied in Eq.(15). Rearranging this inequality and consideration of volume consistency $dV = 0$ during plastic deformation yields the stability condition for rate-independent materials:

$$d_\varepsilon \sigma > \sigma \quad \text{or} \quad d_{\varepsilon_n} \sigma_n > 0 \quad \text{with } \varepsilon = \ln(1 + \varepsilon_n) \text{ and } \sigma = \sigma_n(1 + \varepsilon_n) \quad (16)$$

It states, that the deformation is stable if the slope of the flow curve exceeds the true stress, Eq.(16)₁, or if the slope of the engineering stress-strain curve is greater than zero. Hence, the criterion for instability is defined by equating both sides in Eq.(16)₁ and Eq.(16)₂:

$$d_\varepsilon \sigma = \sigma \quad \text{or} \quad d_{\varepsilon_n} \sigma_n = 0 \quad (17)$$

In the literature, Eq.(17)₁ is often referred to as Considère-criterion [13] for plastic instability and defines the onset of plastic instability and therefore the true necking strain. Eq.(17)₂ is equivalent and indicates, that the nominal necking strain is defined by the maximum of the engineering stress-strain curve, which is widely accepted and corresponds well to observations from experimental quasi-static tensile tests.

4.2 Material with rate-dependent stress-strain relation

With Eq.(17), a criterion defining the onset of non-uniform plastic flow for a material with rate-independent stress-strain relation is available. For a rate-dependent material, which has no well-defined work-hardening rate, this condition cannot be applied [14]. Furthermore, due to thermo-viscoplastic effects (inertia, thermal softening, heat conduction and damage evolution) dynamic necking is a more complex phenomenon than necking in quasi-static boundary conditions. Often, problems in FE simulations concerning the onset of dynamic necking and the plastic deformation behaviour beyond the uniform elongation are explained by the fact, that thermal softening is not considered correctly. Böhm et al. [15] showed, that the classical isothermal approach is just a part of the error, but that taking temperature effects into account still does not yield satisfying results. When evaluating experimental results, the problem arises, that the separation of physical effects and influencing factors is challenging, if not impossible. In contrast, simulations and analytical approaches allow for a specific selection and separate evaluation. Therefore, the attention in this paper is restricted to material with isotropic, strain hardening and rate-dependent properties and we consider only isothermal boundary conditions without the effect of thermal softening. Based on the work of Campbell [14], we derive a criterion for plastic instability considering dynamic conditions by a theoretical analysis of the time variation of strain gradients in a general tensile specimen.

The variations in $A_0(x)$, the initial cross-sectional area along the axis of the specimen, is assumed to be small. The strain gradient in a tensile specimen of any geometry can be defined as the partial derivative of the true strain with respect to the coordinate along the specimen:

$$\lambda(x, t) = \partial_x \varepsilon(x, t) \quad \text{or} \quad \lambda(x, t) = \frac{1}{1+\varepsilon_n(x, t)} \partial_x \varepsilon_n(x, t) \quad (18)$$

Under consideration of Schwarz's theorem, i.e. symmetry of second derivatives, the partial derivative of Eq.(18) with respect to the time t yields:

$$\partial_t \lambda = \partial_x \dot{\varepsilon}(x, t) \quad \text{or} \quad \partial_t \lambda = \frac{1}{1+\varepsilon_n(x, t)} \partial_x \dot{\varepsilon}_n(x, t) - \frac{\dot{\varepsilon}_n(x, t)}{(1+\varepsilon_n(x, t))^2} \partial_x \varepsilon_n(x, t) \quad (19)$$

Where the true strain rate is related to the nominal strain rate by following equation:

$$\dot{\varepsilon} = \frac{1}{1+\varepsilon_n} \dot{\varepsilon}_n \quad (20)$$

Eq.(20) implies, that a constant true strain rate does not imply a constant nominal strain rate and vice versa. Based on Eq.(1), the strain rate for isothermal boundary conditions can be formulated equivalently as a function of true strain and true stress or nominal strain and nominal stress:

$$\dot{\varepsilon} = g(\sigma(x, t), \varepsilon(x, t)) \quad \text{or} \quad \dot{\varepsilon}_n = g_n(\sigma_n(x, t), \varepsilon_n(x, t)) \quad (21)$$

so that

$$d\dot{\varepsilon} = \partial_{\sigma} g d\sigma + \partial_{\varepsilon} g d\varepsilon \quad \text{or} \quad d\dot{\varepsilon}_n = \partial_{\sigma_n} g_n d\sigma_n + \partial_{\varepsilon_n} g_n d\varepsilon_n \quad (22)$$

By substituting of Eq.(22) into Eq.(19), we obtain following ordinary differential equation of first order:

$$\partial_t \lambda + P \lambda = Q \quad (23)$$

with

$$P \equiv -\partial_{\varepsilon} g \quad \text{or} \quad P \equiv \frac{g_n}{1+\varepsilon_n} - \partial_{\varepsilon_n} g_n \quad (24)$$

and

$$Q \equiv \partial_{\sigma} g \partial_x \sigma \quad \text{or} \quad Q \equiv \frac{1}{(1+\varepsilon_n)} (\partial_{\sigma_n} g_n \partial_x \sigma_n) = -\frac{\sigma_n}{A_0(1+\varepsilon_n)} (\partial_{\sigma_n} g_n d_x A_0) \quad (25)$$

From a mathematical point of view it follows from Eq.(23), that the absolute value of the strain gradient $|\lambda|$ increases indefinitely with t unless $P > 0$. That gives the condition for stability in dynamic plasticity under isothermal conditions:

$$\partial_\varepsilon g < 0 \quad \text{or} \quad \partial_{\varepsilon_n} g_n < \frac{g_n}{1+\varepsilon_n} \quad (26)$$

Assuming a static and rate-independent stress-strain curve, i.e. $\dot{\varepsilon}_n = g_n = 0$ and $dg_n = d(e^\varepsilon g) = 0$ respectively, it follows from Eq.(21):

$$d(e^\varepsilon g) = g(de^\varepsilon) + e^\varepsilon(dg) = 0 \quad \text{or} \quad dg_n = \partial_{\sigma_n} g_n d\sigma_n + \partial_{\varepsilon_n} g_n d\varepsilon_n = 0 \quad (27)$$

Substituting Eq.(27) in Eq.(26) and assuming $\partial_\sigma g > 0$ and $\partial_{\sigma_n} g_n > 0$, we get:

$$\partial_\varepsilon \sigma > \sigma \quad \text{or} \quad \partial_{\varepsilon_n} \sigma_n > 0 \quad (28)$$

Hence, the general condition for stability in dynamic plasticity, Eq.(26), reduces to the Considère-criterion respectively the maximum load criterion in Eq.(17) and therefore includes the criterion for static boundary conditions as a special case.

4.3 Application using the Johnson-Cook and Cowper-Symonds model as well as the Overstress hypothesis

Rearranging the isothermal constitutive equations in Eq.(4), Eq.(6), and Eq.(11), the true strain rate may be expressed in the Johnson-Cook model as

$$g^{JC} = \dot{\varepsilon} = \dot{\varepsilon}_0 \cdot \exp \left[\frac{1}{C} \left(\frac{\Delta\sigma}{\sigma_s} \right) \right] \quad \text{or} \quad g_n^{JC} = \dot{\varepsilon}_n = (1 + \varepsilon_n) \cdot \dot{\varepsilon}_0 \cdot \exp \left[\frac{1}{C} \left(\frac{\Delta\sigma_n}{\sigma_{s,n}} \right) \right], \quad (29)$$

in the Cowper-Symonds model as

$$g^{CS} = \dot{\varepsilon} = D \cdot \left(\frac{\Delta\sigma}{\sigma_s} \right)^p \quad \text{or} \quad g_n^{CS} = \dot{\varepsilon}_n = (1 + \varepsilon_n) \cdot D \cdot \left(\frac{\Delta\sigma_n}{\sigma_{s,n}} \right)^p \quad (30)$$

and in the overstress hypothesis as

$$g^{OH} = \dot{\varepsilon} = \tilde{D} \cdot (\Delta\sigma)^p \quad \text{or} \quad g_n^{OH} = \dot{\varepsilon}_n = (1 + \varepsilon_n) \cdot \tilde{D} \cdot ((1 + \varepsilon_n) \cdot \Delta\sigma_n)^p \quad (31)$$

The criterion for instability in dynamic plasticity is given by equating both sides of the inequalities in Eq.(26)₁ or Eq.(26)₂:

$$\partial_\varepsilon g = 0 \quad \text{or} \quad \partial_{\varepsilon_n} g_n = \frac{g_n}{1+\varepsilon_n} \quad (32)$$

For both multiplicative decomposition approaches, the Johnson-Cook and the Cowper-Symonds model, this results under consideration of $\partial_{\varepsilon_n} \sigma_n = 0$ in:

$$\partial_\varepsilon \sigma_s = \sigma_s \quad \text{or} \quad \partial_{\varepsilon_n} \sigma_{s,n} = 0 \quad (33)$$

For the overstress hypothesis, representing an additive decomposition approach, we obtain from Eq.(32):

$$\partial_\varepsilon \sigma_s = \sigma \quad \text{or} \quad (\partial_{\varepsilon_n} \sigma_{s,n}) \cdot (1 + \varepsilon_n) + \sigma_{s,n} = \sigma_n \quad (34)$$

From Eq.(33) and Eq.(34) it can be seen, that the onset of necking is independent of the material parameters that determine the strain rate dependence. For the multiplicative constitutive equations we obtain a, in principle, strain rate-independent constant necking strain and Eq.(34) indicates for the overstress hypothesis, that the dynamic necking strain is always less than the static value.

Fig.3(a) - Fig.3(c) depict the condition for stability applied on the constitutive equations with material parameters from Table 2 and Table 3 in the true stress and true strain representation, whereas Fig.3(d) - Fig.3(f) show the condition for stability in dependence on nominal stress and nominal strain.

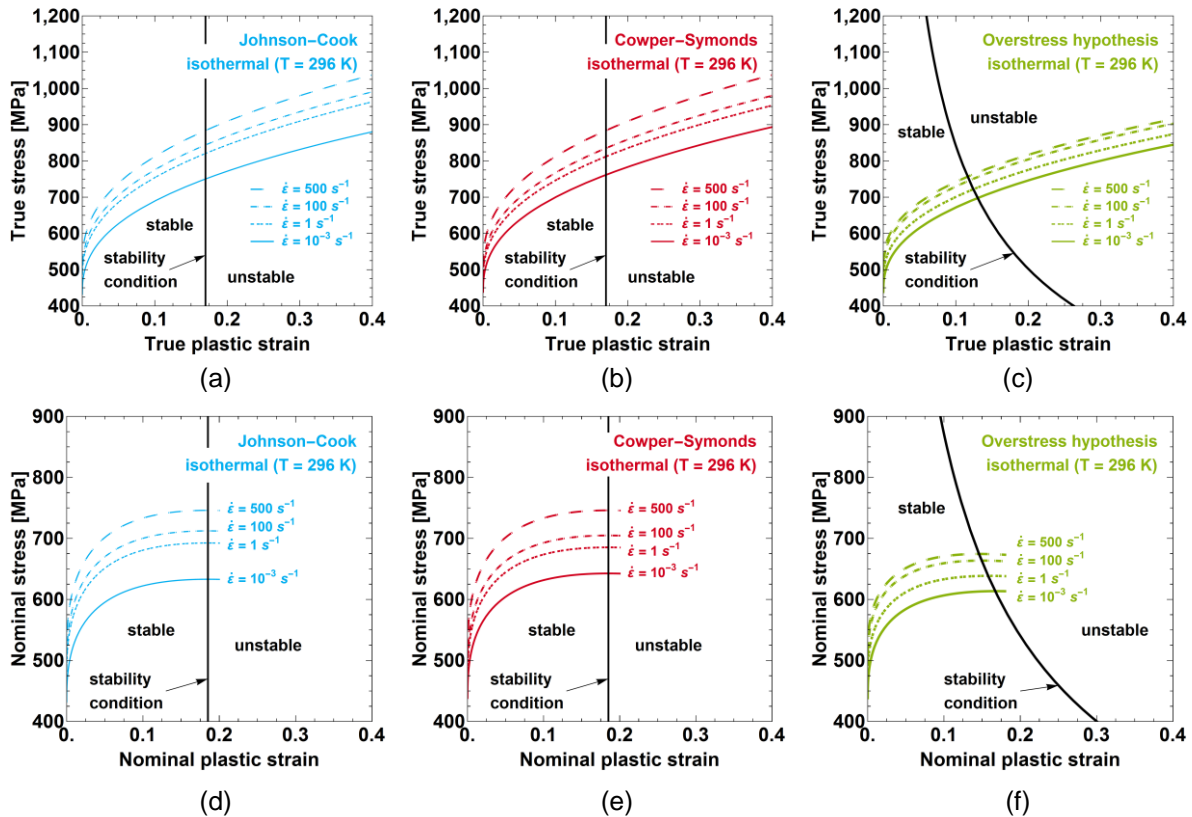


Fig.3: Graphical representation of the stability condition: Johnson-Cook and Cowper-Symonds model, overstress hypothesis in dependence on true stress and true strain (a)-(c) and on nominal stress and nominal strain (d)-(e).

5 Onset of diffuse necking in quasi-static and dynamic tensile tests: Numerical results in comparison to the analytical instability criterion

It is not possible to manufacture ideal specimen, because geometric imperfections as well as material inhomogeneities within a sample cannot be avoided. Therefore, the necking strain found experimentally will always be lower than a theoretical one, derived from analytical approaches. The stability criterion, discussed in the section before, assumed a general tensile specimen with an imperfect geometry, but the variation of initial cross-sectional area was assumed to be small. Considering Eq.(25)₂, a perfect geometry yields $d_x A_0 = 0$, so that $Q = 0$ results. However, the stability condition depends only on the mathematical condition $P > 0$, see Eq.(23), so that the criterion for plastic instability holds even for specimens without geometrical or material imperfections. Fig.4 depicts the FE model of a sheet-metal specimen meshed with shell elements (ELFORM = 2) used for the numerical simulations, which were carried out with LS-DYNA [16].

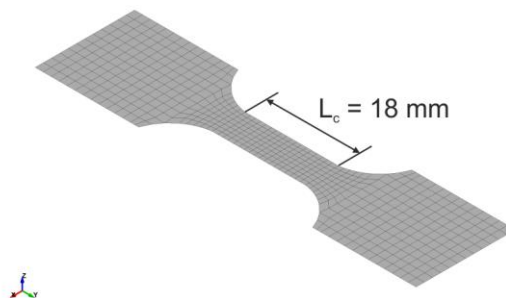


Fig.4: Sheet-metal specimen with rectangular cross-section: Geometry and mesh configuration used for finite element simulations with LS-DYNA

According to the ISO 26203-2 standard [2], the estimated nominal engineering strain rate $\dot{\epsilon}_{n.est}$ can be expressed as the quotient of initial displacement rate v_0 and parallel length of the tensile specimen L_c :

$$\dot{\epsilon}_{n.est} = \frac{v_0}{L_c} \quad (35)$$

The considered specimen geometry is characterised by a parallel length of $L_c = 18$ mm, see Fig.4, so that with chosen nominal strain rates of $\dot{\epsilon}_{n.est} = 10^{-3} s^{-1}$, $1 s^{-1}$, $100 s^{-1}$ and $500 s^{-1}$ and Eq.(35) the velocities summarized in Table 4 result. In the numerical simulations, analogue to experimental tensile tests, the velocities are applied single-sided by a constant displacement rate with fixed opposite edge.

$\dot{\epsilon}_{n.est}$	$10^{-3} s^{-1}$	$1 s^{-1}$	$100 s^{-1}$	$500 s^{-1}$
v_0	0.018 mm/s	18 mm/s	1,800 mm/s	9,000 mm/s

Table 4: Defined constant displacement rates for the numerical simulations

The Johnson-Cook model is defined analytically with *MAT_015 using the material parameters given in Table 2 under consideration of room temperature $T = 296$ K. The Cowper-Symonds model and the overstress hypothesis are applied by using *MAT_024 and defining a table of strain rate-dependent curves of effective stress versus effective plastic strain. The true stress values are calculated by applying Eq.(6) or Eq.(11) in a range of true plastic strain from $0 \leq \epsilon \leq 1$ and using the model parameters given in Table 3. For both, the Cowper-Symonds model as well as the overstress approach, the flow curves are defined for the strain rates $\dot{\epsilon} = \{7.5 \cdot 10^{-4}, 10^{-3}, 0.75, 1, 10, 20, 75, 100, 365, 500, 10^3\} s^{-1}$, which were chosen based on preliminary numerical analyses. In addition, following material parameters for steel were applied in the definitions: Young's modulus $E = 210,000$ MPa, Poisson's ratio $\nu = 0.3$ and mass density $\rho = 7,800$ kg/m³.

For the evaluation and display of numerical results the engineering representation of nominal stress versus nominal strain is used. The calculated tensile force is related to the initial cross-sectional area and the calculated change of length is related to the initial gauge length. In Fig.5(a) - Fig.5(c), the results from the FE simulations of the tensile tests are related to the theoretical stability conditions predicted by Eq.(33)₂ or Eq.(34)₂. The calculated maximum nominal stresses, where $\partial_{\epsilon_n} \sigma_n = 0$ is valid, are shown with squares. It appears, as theoretical predicted, that the onset of plastic instability in the multiplicative models is independent of the strain rate, the calculated necking strain is simulated nearly constant. The simulation results for the overstress hypothesis agree just as well with the predicted instability criterion. With increasing strain rate, the calculated dynamic necking strain decreases with increasing strain rate. The numerical studies showed for the Cowper-Symonds model and the overstress hypothesis that a sufficient quantity of true stress-true strain curves is necessary for a satisfying prediction of the onset of necking with *MAT_024. Comparing the results based on the Johnson-Cook and the Cowper-Symonds models it must be noted, that the plastic deformation behaviour beyond the uniform elongation differs. An evaluation by means of the theoretical approach is not possible and for a further evaluation, the comparison to experimental data is expedient.

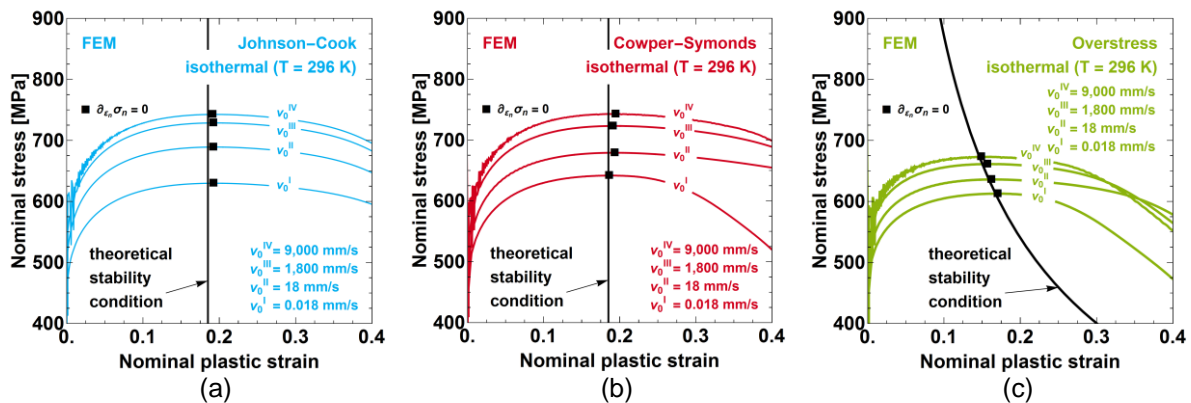


Fig.5: Comparison between theoretical predicted and numerical simulated onset of necking: Johnson-Cook model (a), Cowper-Symonds model (b) and overstress hypothesis (c)

6 Summary

In this paper, a theoretical criterion was derived, describing the condition for plastic instability in rate-dependent materials based on the time variation of the strain gradient in a tensile specimen under isothermal conditions. The analytical stability condition holds even for specimens without geometrical or material imperfections and confirms that the onset of plastic instability is a material characteristic. The influence of multiplicative as well as additive constitutive relations on dynamic necking strains were discussed. For the Johnson-Cook and the Cowper-Symonds model, representing multiplicative approaches, the necking strain is, in principle, predicted to be independent of the strain rate. In contrast, the overstress hypothesis, representing an additive approach, indicates that the dynamic necking strain must decrease with increasing strain rate.

Numerical simulations of dynamic tensile tests with a sheet-metal specimen with rectangular cross-section were performed using LS-DYNA. The derived theoretical stability conditions were related to the results from the FE simulations and it was found that the numerical calculated and the theoretical predicted onset of plastic instability agree very good for the investigated multiplicative and additive approaches. As a result, it may be concluded, that for engineering materials that exhibit a strain rate-dependent necking strain, it is inappropriate to apply multiplicative approaches for the description of the material behaviour in terms of the onset of necking. Here, additive relations are better suited.

In further studies, thermal effects should be considered in the discussion of the theoretical stability criterion and in the numerical simulations. Moreover, in order to evaluate the post-necking behaviour in large deformation problems, the comparison to experimental data from dynamic tensile tests is expedient. Consequently, adiabatic effects must be discussed and the consideration of thermal softening is mandatory.

7 Literature

- [1] ISO 6892-1:2009: "Metallic materials – Tensile testing – Part 1: Methods of test at room temperature", 2009
- [2] ISO 26203-2:2011: "Metallic materials – Tensile testing at high strain rates – Part 2: Servo-hydraulic and other systems", 2011
- [3] Johnson, G. R. ; Cook, W. H.: "A constitutive model and data for metals subjected to large strains, high strain rates and high temperatures". In: Proceedings of the Seventh International Symposium on Ballistics, 1983, 541-547
- [4] Borvik, T. ; Langseth, M. ; Hopperstad, O. ; Malo, K.: "Ballistic penetration of steel plates". In: International Journal of Impact Engineering 22, 1999, 855-886
- [5] Dorogoy, A. ; Rittel, D.: "Determination of the Johnson-Cook Material Parameters Using the SCS specimen". In: Experimental Mechanics 49, 2009, 881-885
- [6] Gambirasio, L. ; Rizzi, E.: "On the calibration strategies of the Johnson-Cook strength model: Discussion and applications to experimental data". In: Material Science & Engineering A 610, 2014, 370-413
- [7] Cowper, G. R. ; Symonds, P. S.: "Strain hardening and strain rate effects in the impact loading of a cantilever beam". Technical Report 28, Brown University, Providence, 1957
- [8] Sokolovsky, V. V.: "Propagation of elasto-viscoplastic waves in bars". In: Prikl. Mat. Mekh. 12, 1948, 261-280
- [9] Malvern, L. E.: "The Propagation of Longitudinal Waves of Plastic Deformation in a Bar of Material Exhibiting a Strain rate Effect". In: Journal of Applied Mechanics 18, 1951, 203-208
- [10] Germanischer Lloyd: "GL II-1-2: Rules for Classification and Construction - II: Materials and Welding - Part 1: Metallic Materials - 2: Steel and Iron Materials". 2009
- [11] Nemat-Nasser, S. ; Guo W. G.: "Thermomechanical response of DH-36 structural steel over a wide range of strain rates and temperatures". In: Mechanics of Materials 35, 2003, 1023-1047
- [12] Joun, M. ; Choi, I. ; Eom, J. ; Lee, M.: "Finite element analysis of tensile testing with emphasis on necking". In: Computational Materials Science 41, 2007, 63-69
- [13] Considère, M.: "L'emploi du fer et Lacier Dans Les Constructions". Annales des Ponts et Chaussées 9, 1885, 574-775
- [14] Campbell, J. D.: "Plastic Instability in Rate-Dependent Materials". In: J. Mech. Phys. Solids 15, 1967, 359-370
- [15] Böhm, R. ; Feucht, M. ; Andrade, F. ; Du Bois, P. ; Haufe, A.: "Prediction of dynamic material failure – Part I: Strain rate dependent plastic yielding". In: Proceeding of the 10th European LS-Dyna Conference 2015, Würzburg, Germany
- [16] Livermore Software Technology Corporation: LS-DYNA Explicit Finite Element Code, Version smp d R8.1.0, Revision 105896